Science of the Total Environment 634 (2018) 1165–1173

Contents lists available at ScienceDirect

Science of the Total Environment

journal homepage: www.elsevier.com/locate/scitotenv

Determining the speciation of Zn in soils around the sediment ponds of chemical plants by XRD and XAFS spectroscopy and sequential extraction

Tatiana Minkina [a], Dina Nevidomskaya [a,*], Tatiana Bauer [a], Victoria Shuvaeva [a], Alexander Soldatov [a], Saglara Mandzhieva [a], Yan Zubavichus [b], Alexander Trigub [b]

[a] *Southern Federal University, Rostov-on-Don 344006, Russia*
[b] *National Research Centre "Kurchatov Institute", Moscow 123182, Russia*

HIGHLIGHTS

- The total content of Zn in Spolic Technosols was about 26,000–66,000 mg/kg.
- Phyllosilicates and Fe-Mn (hydr)oxides are the main stabilizers of Zn mobility.
- A high degree of transformation was detected for the mineral phase in Technosols.
- The EXAFS data in soils revealed 70% of Zn—S bonds and 30% of Zn—O bonds.

GRAPHICAL ABSTRACT

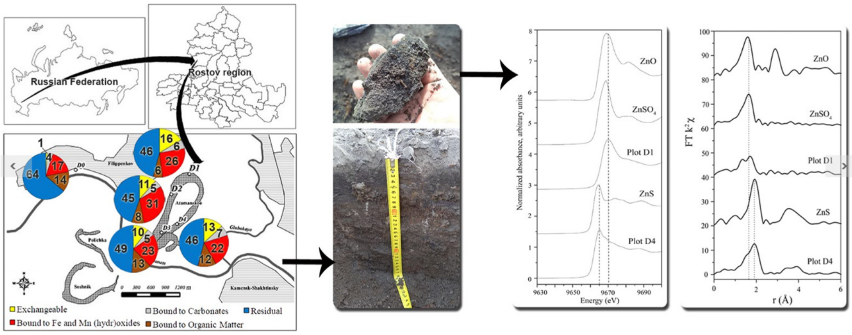

ARTICLE INFO

Article history:
Received 22 August 2017
Received in revised form 6 March 2018
Accepted 8 April 2018
Available online xxxx

Keywords:
Zinc
Spolic Technosols
Fractional composition
Contamination
XANES
EXAFS

ABSTRACT

For a correct assessment of risk of polluted soil, it is crucial to establish the speciation and mobility of the contaminants. The aim of this study was to investigate the speciation and transformation of Zn in strongly technogenically transformed contaminated Spolic Technosols for a long time in territory of sludge collectors by combining analytical techniques and synchrotron techniques. Sequential fractionation of Zn compounds in studied soils revealed increasing metal mobility. Phyllosilicates and Fe and Mn hydroxides were the main stabilizers of Zn mobility. A high degree of transformation was identified for the composition of the mineral phase in Spolic Technosols by X-ray powder diffraction. Technogenic phases (Zn-containing authigenic minerals) were revealed in Spolic Technosols samples through the analysis of their Zn *K*-edge EXAFS and XANES spectra. In one of the samples Zn local environment was formed by predominantly oxygen atoms, and in the other one mixed Zn—S and Zn—O bonding was found. Zn speciation in the studied technogenically transformed soils was due to the composition of pollutants contaminating the floodplain landscapes for a long time, and, second, this is the combination of physicochemical properties controlling the buffer properties of investigated soils. X-ray spectroscopic and X-ray powder diffraction analyses combined with sequential extraction assays is an effective tool to check the affinity of the soil components for heavy metal cations.

1. Introduction

The determination of total content of metals in soil may minimize the risks to biota and human health, assuming that pollutants

---

* Corresponding author.
E-mail address: dnevidomskaya@mail.ru. (D. Nevidomskaya).

https://doi.org/10.1016/j.scitotenv.2018.04.118

transferring to water resources or biota are simply correlated with contamination level (Adamo and Zampella, 2008). For a correct assessment of risk/toxicity of polluted soil, it is crucial to establish the speciation, and mobility of the contaminants. There are several analytical and instrumental methods and strategies that provide information on the behaviour of metals in soil. Chemical methods of sequential extraction are widely used for assessing the forms of metal compounds in soils (Jacquat et al., 2009; Miller et al., 1986; Minkina et al., 2017; Nevidomskaya et al., 2016; Scheinost et al., 2002; Tessier et al., 1979; Wisawapipat et al., 2017; Young et al., 2005). However, the chemical fractionation methods cannot unambiguously identify the speciation of metals at the molecular level because of the limited selectivity of extracts (Burachevskaya et al., 2017; Scheinost et al., 2002). X-ray diagnostic methods – X-ray absorption near edge structure (XANES) and extended X-ray absorption fine structure (EXAFS) – have identified forms of many metals and metalloids in contaminated soils and sediments at the molecular level during the last 30 years (Jacquat et al., 2009; Kirpichtchikova et al., 2006; Manceau et al., 2005; *Synchrotron-based techniques in soils and sediments,* 2010). The leading role of metal-bearing phases was dependent on the source of emission and the type of chemical contamination (Isaure et al., 2005; Juillot et al., 2003; Manceau et al., 2002, 2003; Scheinost et al., 2002). Therefore, it is important to have a concept of metal speciation during the technogenic pedogenesis depending on soil-forming conditions, soil properties, and pollution character.

Studies of Jacquat et al. (2008, 2009) and Degryse et al. (2011), have covered a wide range of soil properties, by combining XAFS spectroscopy and sequential extraction methods. They demonstrated that soil pH and total Zn concentration in the soils are the most important factor for controlling pedogenic Zn speciation. To date, more comparative studies have been performed by combining analytical techniques (Ahnstrom and Parker, 2001; Atkinson et al., 2011; Marzouk et al., 2013) and synchrotron techniques (Diesing et al., 2008; Degryse et al., 2011), to better interpret the metal speciation and reactivity in the soil. The city of Kamensk-Shakhtinskii in Rostov oblast (Russia) is an example of the destructive impact of long-term anthropogenic activity on adjacent land and aquatic ecosystems. The construction of a large industrial centre with chemical plants and production facilities in the city in the 1950s and resulted in the creation of sediment ponds and sludge reservoirs in the Severskii Donets valley. Natural lakes in the Severskii Donets floodplain were used for this purpose. Regular discharge of industrial effluents into these lakes and accidental releases directly to the floodplain landscapes continued up to the mid-1990s. As a result, natural ecosystems were destroyed, and the technogenic lakes by receiving industrial wastes and sludge collectors, were transformed into extremely hazardous sources of secondary environmental contamination. The filtration of entrapped water from settling lakes resulted in the formation of a halo of strongly contaminated groundwater, especially with Zn, under them (Privalenko et al., 2000). In the contaminated zone are deposits of underground fresh water, which are used to supply drinking water to Kamensk-Shakhtinsky town. In this regard, it is important to study the speciation of metals in soils that dictates the intensity of migration and accumulation of metals in soils. The impact of metal-contaminated soils on the entire ecosystem directly depends on metal compounds.

The aim of this study was to observe the accumulation and transformation of Zn in strongly contaminated technogenically transformed soils and the relationships of Zn with organomineral components of the soil matrix by the combination of chemical fractionation and a set of X-ray synchrotron methods.

2. Materials and methods

2.1. Study area

Lake Atamanskoe is located in the Severskii Donets floodplain. This is an oxbow of the Severskii Donets, the main tributary of the Don River (48°20′42.15″N, 40°14′14.46″E). Lake Atamanskoe was used as a reservoir for the industrial wastes released from the chemical plant from the early 1960s to the mid-1990s. The lake contains 180,000 tons of flowing silts, 343,000 tons of low-plastic silts, and >444,000 tons of high-plastic silts (Privalenko et al., 2000). All these sediments are contaminated with HMs and organometallic compounds.

To study the properties, content features, and accumulation of metals, lithological survey of the area adjacent to Lake Atamanskoe were performed in 2015–2017. A geochemical network of 90 monitoring plots was established. Four monitoring plots with high levels of technogenic contamination of soil were selected in the area adjacent to the lake (Fig. 1). According to the World Reference Base of Soil Resources (IUSS Working Group WRB, 2015), all the soil samples from plots D1–D4 were classified as Spolic Technosols. The soil at the monitoring plot D0, situated at 2 km from the Lake, was used as a control, because there was Fluvisol, typical for the studied area (IUSS Working Group WRB, 2015).

2.2. Soil sampling and quality control

Sampling was performed according to ISO 10381-1 (2002). In each monitoring plots, five initial samples were collected from the top layer (0–20 cm depth). The soil sample was made by mixing 5 initial samples collected at one monitoring plot. From each monitoring plots, three soil samples were collected. Samples were stored in polyethylene bags and transported to the laboratory. Soil samples were air dried in special room without chemical reagents at temperature (20–24 °C) and relative humidity 60–70%. The soil was dried to a moisture no >5–6% (the soil is dusty and dry to the touch). Soil samples were grinded up with a pestle and mortar after removing of large particles and plant residues. Then samples were sifted through a 2 mm sieve and homogenized.

The effect of the wetting–drying cycles is common for the soil and cannot significantly affect the Zn speciation in the soil. The upper soil horizons are subjected to regular wetting–drying periods throughout the time of soil existence. On the other hand, it has been shown that trace elements can be mobilized by waterlogging, which makes possible cyclic decreases and increases in extractability (Williams and McLaren, 1982). Soil heterogeneity has a significantly stronger impact on Zn speciation. However, only air-dried samples can be homogenized.

All of the soil samples were previously analyzed and characterized in order to assess the influence of the soil components and properties on heavy metal retention, and to find out how they were distributed in the geochemical phases. The main physical and chemical characteristics of the soil were determined by an accredited analysis laboratory (Accreditation Certificate No. POCC RU 0001.511127) following International Standard ISO Guide 34 (2009) methods.

The soil particle size distribution was determined by the pipette method (with pyrophosphate procedure of soil preparation). In this method carbonates, SOM, Fe, and Al oxides were not removed before the pipette, ISO 13317-2 (2001). The methods used were: for the determination of pH_{water} using a glass electrode in a 1:5 (volume fraction) suspension of soil in water, ISO 10390 (2005); organic matter content by sulfochromic oxidation, ISO 14235 (1998); for carbonates content by using a Scheibler apparatus, ISO 10693 (1995); and determination of exchangeable cations using a hexamminecobalt trichloride solution, ISO 23470 (2011). A mineralogical analysis was performed by immersion microscopy method according to *Methodological Recommendations of the Scientific Council on the Methods of Mineralogical Studies* (2008), which are in line with Russian standards.

The total content of Zn, in the soils was determined by X-ray fluorescent (XRF) scanning spectrometer SPECTROSCAN MAKC-GV (Fifield and Haines, 1997; Kubala-Kukus et al., 2015). The degree of soil contamination with HMs was estimated by comparing with the lithosphere Clarkes (Vinogradov, 1957). The accuracy of Zn content was verified with a reference standard soil sample “Chernozem” no. 29107 spiked with Zn (VNIIM 10.02.012-09/33, KO-163) for X-ray fluorescent

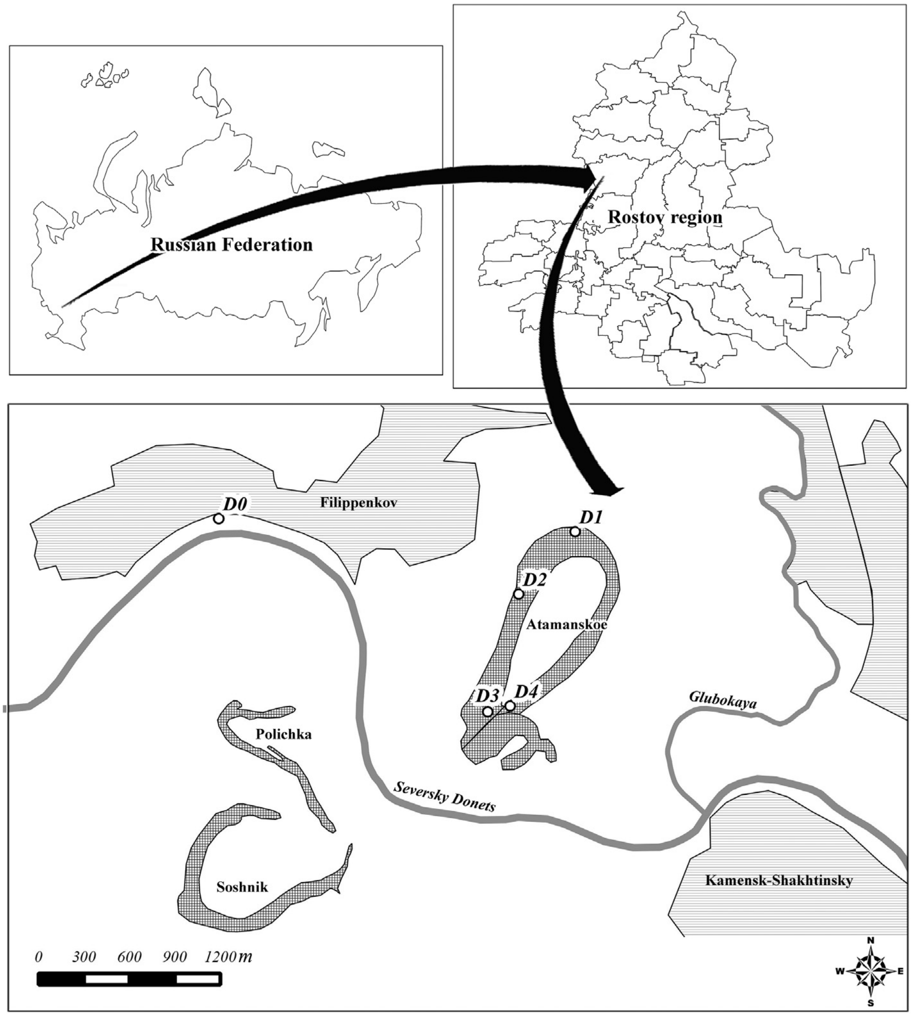

Fig. 1. General scheme of the Lake Atamanskoe region in the industrial zone of the city of Kamensk-Shakhtinskii, Rostov oblast, Russia. Monitoring plots are denoted with circles.

scanning spectrometer like SPECTROSCAN, and standard reference materials of an aqueous solution of Zn for an atomic absorption spectrophotometer. Duplicates and reagent blanks were also used as a part of the quality control. The correctness of the obtained results was repeatedly confirmed by international intercalibrations.

2.2.1. Sequential extraction

The composition of Zn compounds in soils was determined by the sequential fractionation method proposed by Tessier et al. (1979). The methodology published by Tessier et al. (1979) has been cited more than times 1979 to 2017 (Web of Science), which demonstrates the worldwide acceptance of this method's accuracy. This method ensures the separation of five metal fractions: exchangeable (1 M $MgCl_2$), carbonate-bound (1 M CH_3COONa), Fe/Mn (hydr)oxide-bound (0.04 M $NH_2OH\cdot HCl$ in 25% CH_3COOH), organic matter-bound (0.02 M HNO_3 + 30% H_2O_2 (pH 2), then 3.2 M CH_3COONH_4 in 20% HNO_3), and residual (HF + $HClO_4$, then $HNO_{3conc.}$) fractions. The content of Zn in extracts was determined with an atomic absorption spectrophotometer (KVANT 2-AT, Kortec Ltd., Russia).

2.2.2. X-ray absorption spectroscopy

XAFS spectra were collected at the Zn *K*-edge (9659 eV) on the beamline 'Structural Materials Science' (Chernyshov et al., 2009) of the Kurchatov Synchrotron Radiation Source (Kurchatov Institute, National Research Center, Moscow, Russia) with the storage ring operating at 2.5-GeV beam energy and beam currents between 70 and 90 mA (Table 1). All the spectra were recorded under ambient conditions (23 °C) in transmission mode using a channel-cut Si(111) monochromator, which provided energy resolution $\Delta E/E \sim 2 \times 10^{-4}$. The beam spot dimensions were about 0.5 × 0.5 mm. The radiation intensities were measured using two ion chambers filled with appropriate N_2–Ar mixtures in the energy range varied from 200 to 800 eV below and above the Zn *K*-absorption edge, respectively. For each sample, several scans were collected and averaged in order to achieve a higher signal-to-noise ratio.

EXAFS data were analyzed using the Viper (Klementev, 2000, 2001) and IFEFFIT 1.2.11 (Newville, 2001) data analysis packages. All the spectra were normalized, and the atomic background was subtracted from the raw data. The radial pair distribution functions around the Zn atoms were obtained by the Fourier transform of the k^3-weighted EXAFS functions over the range of photoelectron wave numbers 2.6–12.5 Å^{-1}. The structural parameters, including interatomic distances, coordination numbers and Debye–Waller factors, were found

Table 1
Measurement parameters of the beamline "Structural Materials Science", Kurchatov Synchrotron Radiation Source (Chernyshov et al., 2009).

Beamline	Measurement parameters
Beam energy	2.5 GeV
Beam current	70–90 mA
Monochromator	Si(111)
Energy resolution $\Delta E/E$	2×10^{-4}
Spot dimensions	0.5 × 0.5 mm
Data collection mode	Transmission
Detectors	Ion chambers filled with N_2–Ar mixtures

for the first two shells (zinc–oxygen and zinc–sulfur bonding) by the nonlinear fit of theoretical spectra to experimental ones. All possible single and multiple scattering contributions were simulated using the FEFF 7 code (Zabinski et al., 1995).

2.2.3. X-ray powder diffraction

X-ray diffraction patterns were recorded at the Structural Materials Science beamline of the Kurchatov Center for Synchrotron Radiation in transmission geometry using an Image Plate 2D detector and Si monochromator. The wavelength of incident synchrotron radiation was $\lambda = 0.9752$ Å, and the exposure time was 15 min. Intensities were measured over the 5° to 50° 2Θ Bragg angle. A silicon standard (NIST SRM 640C) was used for the angular calibration of the scale.

Experimental and simulated diffraction patterns of standard Zn-containing compounds from the ICSD (Inorganic Crystal Structure Database) were used.

2.3. Statistical analysis

Statistical processing of data from the surveyed monitoring plots was performed using statistical functions of STATISTICA 10.0 software. We used variation statistics methods to calculate arithmetic mean, minimum and maximum values, and confidence interval of the mean. The structural means – mode, median, quartiles, and range – were also determined. The approximation of the empirical distribution by distribution laws was performed in the distribution fitting module of STATISTICA 10.0. Results were considered statistically significant at $p \leq 0.05$.

3. Results and discussion

3.1. Physical and chemical properties of Fluvisol (background soil) and Spolic Technosols

In uncontaminated Fluvisol, the content of organic matter is 3.4 ± 0.1% at pH 7.3 ± 0.2 with insignificant amounts of carbonates found. Data on the content of organic matter in technogenically transformed soils in the plots vary from 2.4 ± 0.1 to 3.6 ± 0.2%. The values of pH in Spolic Technosols were within the range from 7.7 ± 0.1 to 8.0 ± 0.2; the reaction was characterized as weakly and medium alkaline (Table 2).

Spolic Technosols on monitoring plots differ in the distribution of the main particle size fractions. The content of clay particles varies depending on monitoring plots from 17.9 ± 1.5 to 25.4 ± 1.9% (Table 2). The content of sand fractions (1.0–0.05 mm) vary among from 19.9 ± 1.6 to 34.3 ± 2.0%, and silt fractions (0.01–0.001 mm) also varies among the plots from 38.7 ± 2.3 to 46.9 ± 2.8%. Wide variation ranges are observed for the contents of macroelements and Zn in Spolic Technosols (Table 2). The mineralogy of Spolic Technosols includes ilmenite, Fe–Mn hydroxides, pyrite, marcasite, and sulfates (Table 3).

Despite the high contents of total metals in the studied soils, the presence of geochemical barriers (surface and groundwater, vegetation) affects their penetration into adjacent environments. The high content of organic matter in the studied soils represents an organic-sorption barrier. The alkaline reaction in the studied soils favors the formation of metal complexes (chelates) with hydroxyl or mixed hydroxyl–sulfate groups of humic acids (Minkina et al., 2016). The soils with the dominant particle size of clay (<0.001 mm) and silt fractions (0.01–0.001 mm), have an adsorption capacity due to the high degree of dispersion and are, along with organic matter, bearers of properties of a sorption-sedimentation barrier (Perelman and Kasimov, 1999).

The assessment of the studied object revealed a high degree of transformation in the mineral phase of Spolic Technosols, which is characterized by the dominance of authigenic minerals and increased contents of CaO and Fe_2O_3. Zn contamination was observed in all of the samples; lithosphere clarks were exceeded in hundreds of instances (3672.5 ± 304.0–66,075.4 ± 7095.0 mg/kg). Statistical processing data (for 90 monitoring plots) showed that the distribution variability of the variable (total Zn content) did not follow the normal distribution law, and the null hypothesis about the similarity of distributions was rejected. No agreement between the theoretical and empirical distribution frequencies was observed for the total Zn content in the studied soils. The distribution frequency curve is asymmetrical with a shift to the right. The dominant effect on the total Zn content is due to the technogenic factor, which determines the distribution features and high variation of the variable on the monitoring plots.

3.2. Forms of Zn compounds in the Fluvisol (background soil) and Spolic Technosols

Chemical fractionation of Zn compounds on monitoring plot D0 taken as a background plot (Table 4) revealed the dominance of Zn in the residual fraction bound to silicates (64% of the sum of all fractions). Fe–Mn (hydr)oxides also significantly contribute to the strong fixation of Zn: they constitute 17% of the total metal contain (Fig. 2). The similarity in the effective ionic radius of Zn^{2+}, Fe^{2+}, Fe^{3+}, Mg^{2+}, and Al^{3+} allows its incorporation in a large number of soil minerals (Manceau et al., 2005). The relative content of Zn in the first two fractions, which are least strongly bound to the soil, is 5%, including 1% of the most mobile exchangeable forms. The low mobility and dominance of Zn in the

Table 2
Physical and chemical properties Fluvisol (background soil D0) and Spolic Technosols of the investigated monitoring plots.

Sample/parameter		D0	D1	D2	D3	D4
organic matter,%		3.4 ± 0.1	2.8 ± 0.2	3.6 ± 0.2	2.4 ± 0.1	4.4 ± 0.2
pH_{water}		7.3 ± 0.2	7.7 ± 0.1	7.8 ± 0.2	8.0 ± 0.2	7.7 ± 0.3
$CaCO_3$, %		1.3 ± 0.02	7.8 ± 0.2	5.7 ± 0.2	3.8 ± 0.2	5.3 ± 0.3
Exchangeable Ca^{2+}, cmol(+)/kg		31.0 ± 2.4	29.2 ± 2.0	30.0 ± 2.2	27.3 ± 1.9	35.2 ± 1.7
Exchangeable Mg^{2+}, cmol(+)/kg		4.5 ± 0.3	4.8 ± 0.1	5.1 ± 0.1	4.3 ± 0.1	5.0 ± 0.2
Sand fractions (1.0–0.05 mm), %		13.8 ± 0.9	34.3 ± 2.0	22.2 ± 1.5	19.9 ± 1.6	28.3 ± 1.6
Silt fractions (0.01–0.001 mm). %		53.8 ± 4.2	46.9 ± 2.8	59.9 ± 4.4	54.7 ± 4.1	38.7 ± 2.3
Clay fraction (<0.001 mm), %		32.4 ± 2.1	18.8 ± 1.6	17.9 ± 1.5	25.4 ± 1.9	33.0 ± 2.6
Material (chemical) composition, %	SiO_2	62.8 ± 7.1	61.1 ± 4.1	62.3 ± 4.3	54.8 ± 3.0	54.8 ± 5.4
	Al_2O_3	14.7 ± 0.6	15.0 ± 0.8	14.1 ± 0.8	11.3 ± 0.5	11.8 ± 0.7
	Fe_2O_3	7.5 ± 0.3	7.9 ± 0.1	9.0 ± 0.05	7.7 ± 0.3	6.0 ± 0.1
	CaO	3.2 ± 0.1	3.6 ± 0.05	2.8 ± 0.002	11.1 ± 1.1	11.7 ± 1.0
	MgO	1.5 ± 0.09	1.3 ± 0.03	1.1 ± 0.01	4.5 ± 0.6	2.0 ± 0.1
	K_2O	2.1 ± 0.08	1.9 ± 0.03	2.1 ± 0.05	1.9 ± 0.001	1.4 ± 0.2
	P_2O_5	0.2 ± 0.02	0.2 ± 0.003	0.2 ± 0.01	0.3 ± 0.01	0.2 ± 0.001
	SO_3	0.03 ± 0.003	4.3 ± 0.03	5.6 ± 0.02	7.1 ± 0.1	7.3 ± 0.1
	Na_2O	1.0 ± 0.04	0.9 ± 0.02	0.8 ± 0.04	0.8 ± 0.01	0.9 ± 0.03
Total Zn content, mg/kg	Zn (83*)	90.0 ± 7.6	**25,973.7 ± 1780.5**	**13,672.5 ± 304.0**	**66,075.4 ± 7095.0**	**62,032.1 ± 5903.0**

(*) lithosphere clark (Vinogradov, 1957); excesses over the clarks are highlighted in bold.

Table 3
Mineralogy composition Fluvisol (background soil D0) and Spolic Technosols of the investigated monitoring plots, %.

Sample	Terrigenic minerals								Autigenic minerals			
	Stable	Intermediate		Unstable								
	Ilmenite	Rutil	Zircon	Staurolite	Amphibole	Muscovite, biotite	Magnetite, hematite	Pyroxene	Iron hydroxides	Pyrite, marcasite	Carbonates	Sulfates
D0	5.0	4.0	8.0	4.0	nd[b]	nd	57.0	3.0	13.0	1.0	tr	5.0
D1	8.0	tr[a]	tr	nd	3.0	2.0	2.0	0.5	13.0	8.0	9.0	54.5
D2	10.0	tr	tr	nd	nd	nd	3.0	nd	15.0	15.0	2.0	55.0
D3	6.0	tr	tr	nd	nd	nd	tr	nd	30.0	8.0	6.0	50.0
D4	12.0	tr	tr	nd	nd	nd	tr	nd	20.0	8.0	tr	60.0

[a] (tr) traces.
[b] (nd) not detected.

residual fraction confirm the absence of significant amounts of technogenic metal in the background soil. In the uncontaminated (background) soil, the following distribution of Zn among the compounds forms is revealed: residual fraction > Fe–Mn (hydr)oxide-bound fraction > organic matter-bound fraction > carbonate-bound fraction > exchangeable fraction.

In highly contaminated technogenic soils, an increase in the absolute content of Zn compounds is revealed in all fractions (Table 4). The metal content increased in the exchangeable fraction and the fractions bound to Fe and Mn oxides and carbonates, which increased their relative contents to 15%, 14%, and 3%, respectively (Fig. 2). The alkaline reaction of the medium, the presence of organic matter, and the high degree of dispersion in the studied soils reduced the mobility of Zn and limited the environmental risks for biological absorption.

In soils on monitoring plots D1–D4, the residual fraction is dominant; it makes up 45% (D2) to 49% (D3) of total metal content (Fig. 2). Clay minerals have high sorption capacity for Zn (Jacquat et al., 2009; Manceau et al., 2002). Possibility of Al substitution by Zn cations in the octahedral structure of phyllosilicates was proved by the synchrotron radiation method (Myers and Thorbjornsen, 2004).

Along with the residual fraction, the fraction of Fe and Mn (hydr)oxides fixed 22 to 31% of Zn (Table 4, Fig. 2). It was not an increase in Zn affinity for the reaction centres of iron minerals. An abrupt increase in the content of metals in the amorphous Fe fraction compared to the crystalline Fe fraction can be indicative of the technogenic component of soil contamination (Pinskii et al., 2010). Despite the high activity of Mn oxides for the adsorption of metals in the soil (Michálková et al., 2016), their role in the fixation of metal in the studied soils is insignificant because of their low content (230–1167 mg/kg) (Table 4). The Zn ion is accommodated in octahedral structures in (hydr)oxides and forms both inner- and outer-sphere complexes on the adsorbent surface (Minkina et al., 2014). The presence of sorption barriers in the studied soils in the absence of permanent contamination hampered the metal mobility; therefore, the content of the exchangeable fraction under this high level of contamination varies from 10 to 16%. This is confirmed by the data (Minkina et al., 2017) about the high mobility of Zn in technogenically disturbed soils adjacent to the Karabashmed copper smelter, where the content of exchangeable Zn forms is 13–24% of its total amount. Low pH values (3.9–4.4) and C_{org} content (0.4–0.6%), as well as the dominance of sand fractions in soil particle-size distribution, also contribute.

The fraction bound to organic matter makes up 6 to 13% (Fig. 2). The insignificant role of soil organic matter in the fixation of Zn is related to its highest affinity with iron minerals (Arenas-Lago et al., 2014; Li and Thornton, 2001; Minkina et al., 2016; Nannoni et al., 2011; Shaheen et al., 2015). Metals have a low ability to form stable chelate complexes with organic matter (Pinskii and Minkina, 2013). This is confirmed by the stability constants of metal complexes with humic acids at pH 7 (Kabata-Pendias, 2011): the stability constant was 10.3 and 12.3 for Zn and Cu (which has a high organophylicity). The content of the carbonate-bound fraction is the lowest and does not exceed 7% (Table 4, Fig. 2). The analysis of XANES spectra for *K*-edge of Zn absorbed by the carbonate phase showed that the Zn ions replace the Ca ions in the octahedric positions and display 1s → 4p electronic transition (Minkina et al., 2014). Moreover, they are coordinated with carbonate ions as ligands, forming absorbed complexes at the surface of mineral calcite.

The distribution of Zn among the fractions is changed compared to the background soil: residual fraction > Fe–Mn (hydr)oxide-bound fraction > exchangeable fraction ≥ organic matter-bound fraction > carbonate-bound fraction.

The comparison of diffraction patterns (Fig. 3) revealed that quartz is the dominant phase in the soil of plot D1; a significant amount of calcite is found, along with quartz, in the Spolic Technosols of plot D4. The diffraction patterns of both samples also contain diffraction peaks corresponding to crystalline components from the group of phyllosilicates: hydromuscovite (illite), kaolinite, gibbsite and smectites with the montmorillonite mineral phase as an example.

The sensitivity of the XANES spectra to the geometry of bonds can be used for the preliminary qualitative estimation of the molecular structural state of local Zn surrounding in soil samples. The XANES spectra of Zn for several standard compounds with the known structure of Zn—S (ZnS) and Zn—O (ZnO and $ZnSO_4$) bonds show a significant difference in the position of the absorption edge, which makes it possible to discriminate these types of Zn surrounding in soil samples. The XANES spectra of Zn (Fig. 4) for the soil of monitoring plot D1 show a similarity to the standard spectra, in which Zn is coordinated to oxygen (ZnO, $ZnSO_4$), where the main absorption peak is at ~9670 eV. The XANES spectrum of soil sample from plot D4 is close to that of ZnS, and its main absorption peak is at ~9665 eV. This agrees with the results of a mineralogical analysis, which revealed the dominance of authigenic sulfates (Table 2) formed during the long-term (up to 57 years)

Table 4
Fractional composition of Zn compounds (mg/kg) in Fluvisol (background soil D0) and Spolic Technosols of the investigated monitoring plots.

Monitoring plot	Fractions				
	Exchangeable	Carbonate-bound	Fe/Mn (hydr)oxide-bound	Organic matter-bound	Silicate-bound (residual)
D0	0.6 ± 0.2	3.6 ± 0.7	15.4 ± 1.3	12.6 ± 0.9	57.8 ± 4.7
D1	4193.2 ± 674.1	1527.3 ± 195.3	6682.0 ± 97.0	1648.7 ± 190.1	11,916.2 ± 1891.0
D2	1537.8 ± 182.5	715.7 ± 9.5	4205.2 ± 3.8	1131.9 ± 15.6	6081.9 ± 198.3
D3	6867.2 ± 786.0	3456.8 ± 6.9	15,039.4 ± 1053.4	8540.2 ± 1890.1	32,172.0 ± 3110.7
D4	8254.3 ± 900.9	4578.9 ± 0.399.0	15,421.6 ± 1570.3	7580.9 ± 1325.6	28,196.4 ± 3948.5

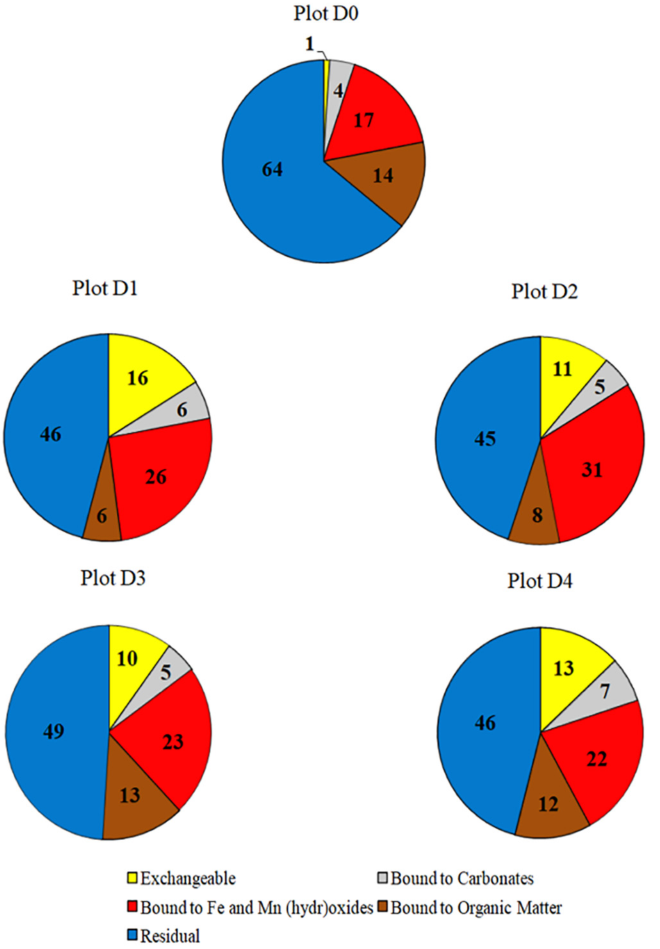

Fig. 2. Fractional composition of Zn in Fluvisol (D0) and Spolic Technosols, % of total content.

technogenic contamination. In the soil sample from monitoring plot D4, higher energy features are also detected, which indicate that mixed Zn—S and Zn—O bonds can form in the sample. Obviously, in this case the main influence on the molecular-structural state of Zn in soils is produced by qualitative changes in the absorption of heavy metals: the state of its material and mineralogical compositions.

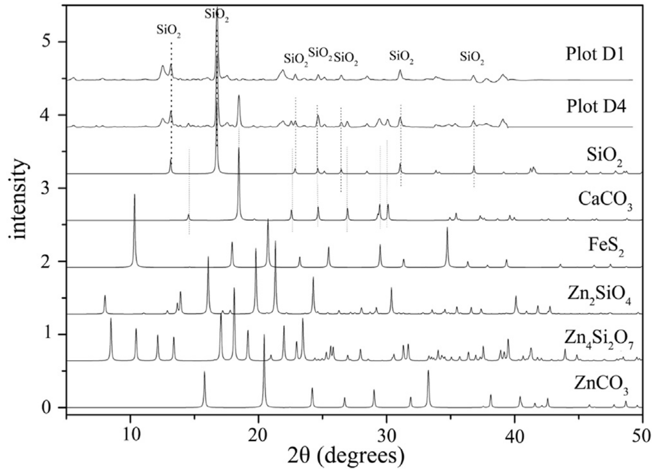

Fig. 3. Experimental powder X-ray diffraction patterns for Spolic Technosols samples compared to the simulated X-ray diffraction patterns of compounds selected from the ICSD database.

Zn K-EXAFS spectra in the *k* and R spaces for soil samples in comparison with the standard spectra of minerals $ZnSO_4$, ZnO (sphalerite) and ZnO (zincite) are shown in Figs. 5 and 6. In zincite, Zn atoms are tetrahedrally coordinated by O atoms (first coordination sphere) with an average bond length of 1.98 Å; in addition, each Zn atom is surrounded by 12 neighbouring Zn atoms at an average distance of 3.23 Å (Albertsson et al., 1989). Thus, two peaks observed on the radial distribution function for zincite at 1.5 and 2.9 Å (Fig. 5) correspond to the Zn—O and Zn—Zn distances, respectively. In $ZnSO_4$, Zn is coordinated by four O atoms and only two Zn atoms. The Zn—Zn distance is 3.36 Å; there are two different short Zn—O bonds (1.95 and 2.04 Å). The spectrum of $ZnSO_4$, as well as the spectrum of ZnO, has a peak of the Zn—O bond; however, the second peak (Zn—Zn bond) is almost absent because of the low coordination number. The Zn—S bond is 2.34 Å в ZnS, which is longer than the Zn—O bonds in ZnO and $ZnSO_4$ by 0.2–0.3 Å; therefore, the peak corresponding to the Zn—S bond is observed at a longer distance in the Fourier-transformed XAFS spectrum (Fig. 5). This obvious difference indicates that the Zn—S and Zn—O molecular structural bonds are significantly different in soil samples D1 and D4. Jacquat et al. (2008, 2009) showed that, with increasing soil pH, specific sorption of Zn to organic matter, phyllosilicates, metal oxides, and carbonates becomes more relevant. Moreover, the formation of Zn precipitates as zincite (ZnO), Zn hydroxide ($Zn(OH)_2$), smithsonite ($ZnCO_3$)

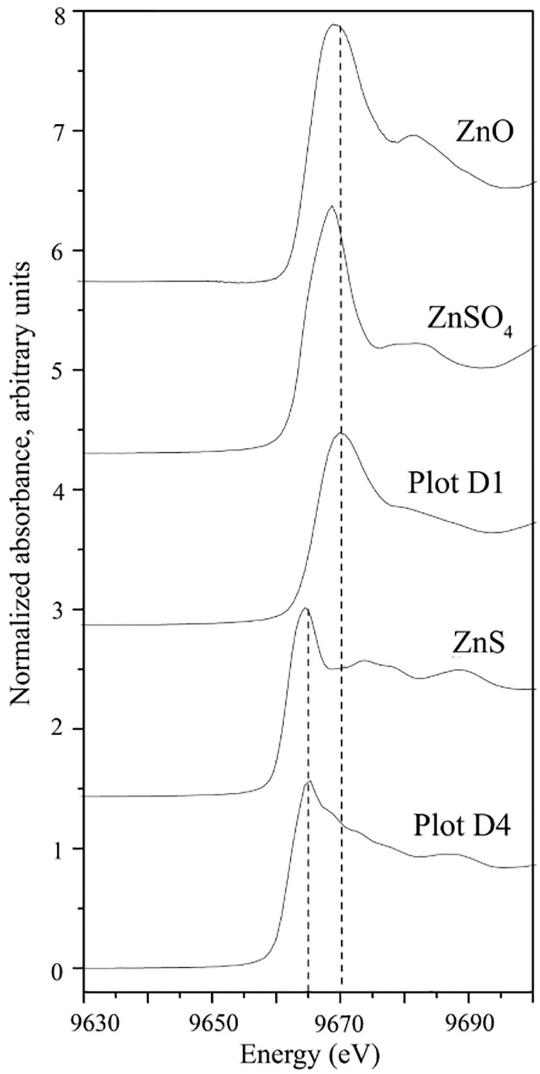

Fig. 4. Background corrected and normalized X-ray absorption near edge structure (XANES) spectra at the Zn *K*-edge for Spolic Technosols samples and selected standards.

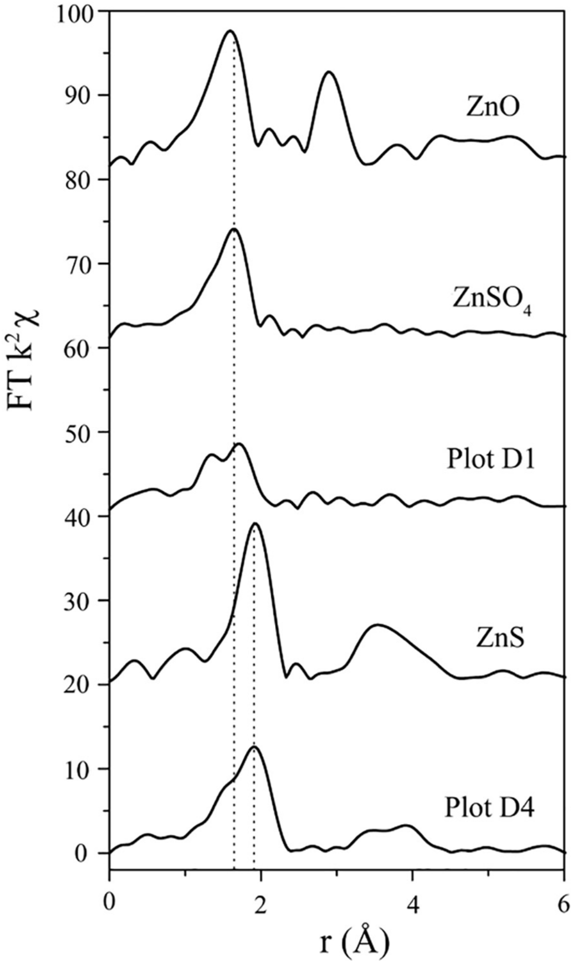

Fig. 5. k^2-weighted EXAFS oscillations extracted from the Zn *K*-edge absorption spectra Spolic Technosols samples and selected standards.

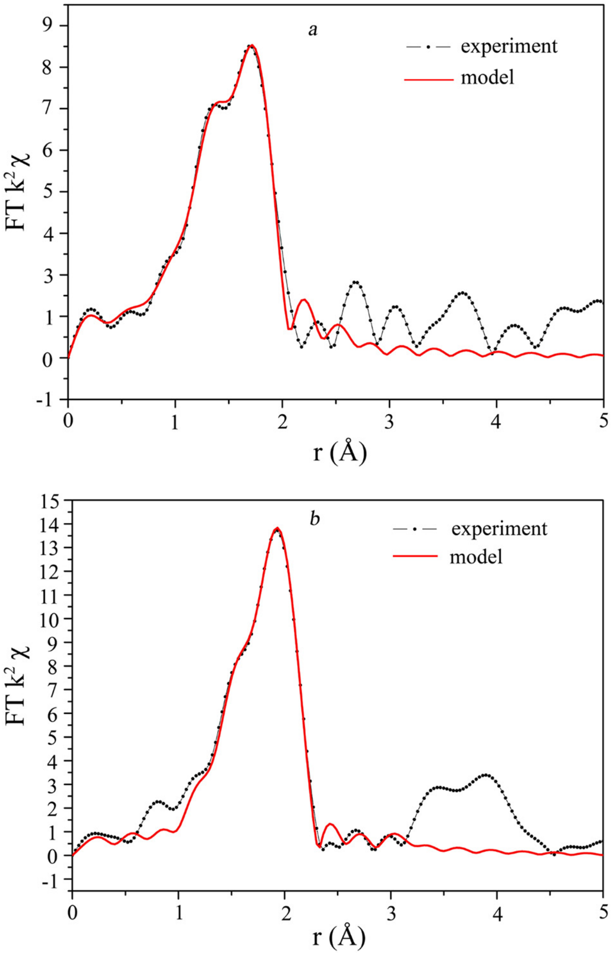

Fig. 6. The best fits of the XAFS FT for Spolic Technosols samples (*a*) D1 and (*b*) D4 (the experimental data are shown by the black line and the fits to the data are shown by the red line). (For interpretation of the references to colour in this figure legend, the reader is referred to the web version of this article.)

and hydrozincite ($Zn_5(OH)_6(CO_3)_2$) in alkaline conditions can decrease Zn solubility.

It has been found that new technogenic phases (Zn-containing phyllosilicates) form in strongly contaminated soils (Juillot et al., 2003; Manceau et al., 2005; Schlegel et al., 2001). In the aluminosilicate-bound (residual) fraction, layered Zn phases were revealed (Manceau et al., 2003, 2004; Scheinost et al., 2002), and the mechanism of Zn entering into the octahedral structures of layered minerals was determined. These regularities revealed using the XANES and EXAFS techniques agree with the results of the chemical fractionation of Zn in the studied soils. The affinity of clay minerals to HMs cations is due to their high surface energy and reactivity related to the small size of particles and their morphological elements, as well as the specific properties of HMs cations determined by the electron structure of their atoms (Pinskii, 1998). The increased concentration of Zn in soils and sediments with the dominant particle-size of clay (<0.001 mm) and silt fractions (0.01–0.001 mm) is related to the high sorption capacity of clay minerals (Guisti, 2011; Myers and Thorbjornsen, 2004), although the portion of zinc strongly fixed in the lattice of clay minerals is unknown. The sufficiently high content of organic matter (Table 4) favors the interaction of Zn^{2+} ions with humic acids of chernozem, which coordinate with functional groups and ligands to form tetrahedral Zn coordinations (Voegelin et al., 2005). The finely dispersed fractions (soil particles <0.01 mm) of Technosols significantly affects the surface properties of mineral components of the solid phase, as well as its adsorption capacity and buffering properties due to the formed mineral–organic compounds with Zn (Fedotov et al., 2007; Petruzzelli et al., 1997).

The XANES and Fourier-transformed *K*-edge EXAFS spectra of Zn in two Spolic Technosols samples show obvious differences (Fig. 6a, b), which confirm the different speciations of Zn in these samples. The Fourier-transformed EXAFS spectrum for soil sample D1 is more similar to the analogous spectrum of $ZnSO_4$, although it contains an additional intense peak at lower R. The absence of the peak corresponding to the second coordination sphere (Zn—Zn) indicates that ZnO is not the dominant component of the sample. In the Technosols of monitoring plot D4, the main peaks in the Fourier-transformed EXAFS spectrum correspond to sphalerite, which is indicative of the dominance of Zn—S bonds. However, an additional feature at lower R is indicative of the presence of Zn—O bonding in the sample. It has been shown (Voegelin et al., 2005) that, when the soil is contaminated with zincite, ZnO is transformed and mainly enters into Zn-containing trioctahedral structures (up to 64% during the first year). In Ontario (Canada), the soils with moderate and increased amounts of Zn also contain an increased content of sulfur: 3.5–9.5 g S/kg. The determination of the redox status of sulfur by XANES analysis showed that 35–45% of the total sulfur occurs in the most reduced state, in the form of sulfides and thiols (Martinez et al., 2002). Synchrotron micro X-ray diffraction analysis revealed sphalerite ZnS in soil microzones. The interactions of Zn with organic matter are uncertain. X-ray absorption spectroscopy in organic soils proved the formation of stable organic Zn compounds: $Zn(CH_3COO)_2$ and Zn-arginate (Bazilevskaya and Lanzirotti, 2006). The best fits were achieved assuming two Zn—O shells for D1 and mixed Zn—S and Zn—O bonding for the D4 (Table 5). The Zn—O

Table 5
Best-fit results of Zn K edge EXAFS data for Zn in technogenically disturbed soils (Spolic Technosols).

Sample	Shell	R (Å)	σ^2 (Å^2)	CN	ΔE (eV)	R-factor (%)	k range (Å^{-1})	R range (Å)
D1	Zn—O$_1$	1.92	0.007	2.32	−0.77	3.53	2.13–12.65	1–2
	Zn—O$_2$	2.10	0.007	5.05	−0.77			
D4	Zn—O$_1$	2.01	0.008	2.25	2.16	3.3	2.66–13.25	1.34–2.33
	Zn—S	2.34	0.007	4.6	2.16			

bond lengths for D1 samples are closer to those of $ZnSO_4$ (1.95–2.04 Å) than to ZnO. The estimations based on the Zn—S and Zn—O coordination numbers for the soil D4 show that it contains about 70% Zn—S bonds and 30% Zn—O bonds. According to the results obtained for the upper horizon of strongly contaminated soils in Palmerton (Scheinost et al., 2002), the dominant fixation of Zn was due to sulfide (sphalerite). Prospects for research in the field of geochemistry of anthropogenic landscapes should be based on the studying of the molecular-structural state of objects, and not just chemical elements. Studies by XAFS/XRD are good methods for complementing and verifying the sequential extraction results. Combining them is an effective tool to check the affinity of the soil components for heavy metal cations.

4. Conclusions

The regularities of the accumulation and transformation of Zn in strongly contaminated technogenically transformed soils were revealed by a combination of chemical fractionation and a set of X-ray synchrotron methods. Several hundred-fold excesses of the lithosphere clark for Zn were detected in the studied soils located in the area of collecting pond for industrial waste from the chemical plant. Speciation forms of Zn in the studied soil samples were identified. It was found that metal mobility increases in technogenically contaminated soils. However the highest Zn content is associated with the least available soil fractions. Phyllosilicates and Fe/Mn (hydr)oxides are the main stabilizers of metal mobility. The relative distribution of Zn compounds among the fractions in the studied Spolic Technosols is as follows: residual fraction > Fe–Mn (hydr)oxide bound fraction > exchangeable fraction ≥ organic matter-bound fraction > carbonate-bound fraction.

The residual fraction of the technogenically transformed soils, contains the highest proportion of Zn (45–49%), indicating that the most form of Zn is strongly retained in the soil. A high degree of transformation was revealed for the composition of the mineral phase in Spolic Technosols, which is dominated by authigenic minerals. Hypergenic changes in the mineral–organic matrix of Spolic Technosols revealed different surrounding types of Zn, which is the dominant pollutant metal in the studied soils. The fitting results of the EXAFS data revealed 70% of Zn—S bonds and 30% of Zn—O bonds. It is suggested that fixation of Zn in scarcely available forms with Zn—O and Zn—S bonds occurs under alkaline conditions and high content of sulfate ions of the studied Spolic Technosols, which reduces the mobility of Zn and restricts the environmental risks of biological uptake.

The application of X-ray absorption spectroscopy methods (XANES and EXAFS) in combination with extractive fractionation in soils of other places in Russia and the world enables the researcher to obtain comprehensive information on the state of metals in contaminated soils, interaction between the metal and soil components, phases containing the metals in the soils, and the strength of bonds between these phases and metals. Further coupled application of conventional chemical techniques and modern physical instrumental methods will significantly widen the understanding of the mechanisms of chemical transformations of heavy metals in soils.

Acknowledgements

The work was supported by the Russian Science Foundation, project no. 16-14-10217.

References

Adamo, P., Zampella, M., 2008. Chemical speciation to assess potentially toxic metals' (PTMs') bioavailability and geochemical forms in polluted. In: De Vivo, B., Belkin, H.E., Lima, A. (Eds.), Environmental Geochemistry Site Characterization, Data Analysis and Case Histories. Elsevier:pp. 175–212 https://doi.org/10.1016/B978-0-444-53159-9.00009-7.

Ahnstrom, Z.A.S., Parker, D.R., 2001. Cadmium reactivity in metal-contaminated soils using a coupled stable isotope dilution-sequential extraction procedure. Environ. Sci. Technol. 35, 121–126.

Albertsson, J., Abrahams, S.C., Kvick, A., 1989. Atomic displacement, anharmonic thermal vibration, expansivity, and pyroelectric coefficient thermal dependences in ZnO. Acta Crystallogr. 45, 34–40.

Arenas-Lago, D., Andrade, M.L., Lago-Vila, M., Rodríguez-Seijo, A., Vega, F.A., 2014. Sequential extraction of heavy metals in soils from a copper mine: distribution in geochemical fractions. Geoderma 230-231, 108–118.

Atkinson, N.R., Bailey, E.H., Tye, A.M., Breward, N., Young, S.D., 2011. Fractionation of lead in soil by isotopic dilution and sequential extraction. Environ. Chem. 8, 493–500.

Bazilevskaya, K.A., Lanzirotti, A., 2006. Zinc coordination to multiple ligand atoms in organic-rich surface soils. Environ. Sci. Technol. 40, 5688–5695.

Burachevskaya, M.V., Minkina, T.M., Mandzhieva, S.S., Bauer, T.V., Chaplygin, V.A., Sushkova, S.N., Orlović-Leko, P., Mashtykova, Yu, L., Rajput, V.D., 2017. Comparing two methods of sequential fractionation in the study of copper compounds in Haplic Chernozem under model experimental conditions. J. Soils Sediments https://doi.org/10.1007/s11368-017-1711-7.

Chernyshov, A.A., Veligzhanin, A.A., Zubavichus, Y.V., 2009. Structural materials science end-station at the Kurchatov synchrotron radiation source: recent instrumentation upgrades and experimental results. Nucl. Inst. Methods Phys. Res. A 603, 95–98.

Degryse, F., Voegelin, A., Jacquat, O., Kretzschmar, R., Smolders, E., 2011. Characterization of zinc in contaminated soils: complementary insights from isotopic exchange, batch extractions and XAFS spectroscopy. Eur. J. Soil Sci. 62, 318–330.

Diesing, W.E., Sinaj, S., Sarret, G., Manceau, A., Flura, T., Demaria, P., Siegenthaler, A., Sappin-Didier, V., Frossard, E., 2008. Zinc speciation and isotopic exchangeability in soils polluted with heavy metals. Eur. J. Soil Sci. 59, 716–729.

Fedotov, G.N., Pakhomov, E.I., Pozdnyakov, A.I., Kuklin, A.I., Islamov, A.K., Putlyaev, V.I., 2007. Structure and properties of soil organic-mineral gel. Eurasian Soil Sci. 40, 956–961.

Fifield, F.W., Haines, P.J., 1997. Environmental Analytical Chemistry. Blackie Academia & Professional, London, UK.

Guisti, L., 2011. Heavy metals in urban soils of Bristol (UK). Initial screening for contaminated land. J. Soils Sediments 11, 1385–1398.

Isaure, M.-P., Manceau, A., Geoffroy, N., Laboudigue, A., Tamura, N., Marcus, M.A., 2005. Zinc mobility and speciation in soil covered by contaminated dredged sediment using micrometer-scale and bulk-averaging X-ray fluorescence, absorption and diffraction techniques. Geochim. Cosmochim. Acta 69, 1173–1198.

ISO 10381-1, 2002. Soil quality. Sampling. Part 1. Guidance on the Design of Sampling Programmes.

ISO 10390, 2005. Soil Quality – Determination of pH.

ISO 10693, 1995. Soil Quality – Determination of Carbonate Content – Volumetric Method.

ISO 13317-2, 2001. Determination of Particle Size Distribution by Gravitational Liquid Sedimentation Methods – Part 2: Fixed Pipette Method.

ISO 14235, 1998. Soil Quality – Determination of Organic Carbon by Sulfochromic Oxidation.

ISO Guide 34, 2009. General Requirements for the Competence of Reference Material Producers.

ISO NF EN 23470, 2011. Soil Quality – Determination of Effective Cation Exchange Capacity (CEC) and Exchangeable Cations.

IUSS Working Group WRB, 2015. World reference base for soil resources 2014, update 2015. International soil classification system for naming soils and creating legends for soil maps. World Soil Resources Reports No. 106. FAO, Rome.

Jacquat, O., Voegelin, A., Villard, A., Marcus, M.A., Kretzschmar, R., 2008. Formation of Zn-rich phyllosilicate, Zn-layered double hydroxide and hydrozincite in contaminated calcareous soils. Geochim. Cosmochim. Acta 72, 5037–5054.

Jacquat, O., Voegelin, A., Kretzschmar, R., 2009. Soil properties controlling Zn speciation and fractionation in contaminated soils. Geochim. Cosmochim. Acta 73, 5256–5272.

Juillot, F., Morin, G., Ildefonse, P., Trainor, T.P., Benedetti, M., Galoisy, L., Calas, G., Brown, G.E., 2003. Occurrence of Zn/Al hydrotalcite in smelter-impacted soils from northern France: evidence from EXAFS spectroscopy and chemical extractions. Am. Mineral. 88, 509–526.

Kabata-Pendias, A., 2011. Trace Elements in Soil and Plants. CRC Press, Boca Raton.

Kirpichtchikova, T.A., Manceau, A., Spadini, L., Panfili, F., Marcus, M.A., Jacquet, T., 2006. Speciation and solubility of heavy metals in contaminated soil using X-ray microfluorescence, EXAFS spectroscopy, chemical extraction, and thermodynamic modeling. Geochim. Cosmochim. Acta 70, 2163–2190.

Klementev, K.V., 2000. Package “VIPER (visual processing in EXAFS researches) for Windows”. Nucl. Inst. Methods Phys. Res. A 448, 299–301.

Klementev, K.V., 2001. Extraction of the fine structure from X-ray absorption spectra. J. Phys. D 34, 209–217.

Kubala-Kukus, A., Banas, D., Braziewicz, J., Dziadowicz, M., Kopec, E., et al., 2015. X-ray spectrometry and X-ray microtomography techniques for soil and geological samples analysis. Nucl. Inst. Methods Phys. Res. B 364, 85–92.

Li, X., Thornton, I., 2001. Chemical partitioning of trace and major elements in soils contaminated by mining and melting activities. Appl. Geochem. 16, 1693–1706.

Manceau, A., Marcus, M.A., Tamura, N., 2002. Quantitative speciation of heavy metals in soils and sediments by synchrotron X-ray techniques. In: applications of synchrotron radiation in low-temperature geochemistry and environmental science. Rev. Mineral. Geochem. 49, 341–428.

Manceau, A., Tamura, N., Celestre, R.S., Macdowell, A.A., Geoffroy, N., Sposito, G., Padmore, H.A., 2003. Molecular-scale speciation of Zn and Ni soil ferromanganese nodules from loess soils of the Mississippi Basin. Environ. Sci. Technol. 37, 75–80.

Manceau, A., Marcus, M.A., Tamura, N., Proux, O., Geoffroy, N., Lanson, B., 2004. Natural speciation of Zn at the micrometer scale in a clayey soil using X-ray fluorescence, absorption, and diffraction. Geochim. Cosmochim. Acta 68, 2467–2483.

Manceau, A., Tommaseo, C., Rihs, S., Geoffroy, N., Chateigner, D., Schlegel, M., Tisserand, D., Marcus, M.A., Tamura, N., Chen, Z.S., 2005. Natural speciation of Mn, Ni, and Zn at the micrometer scale in a clayey paddy soil using X-ray fluorescence, absorption, and diffraction. Geochim. Cosmochim. Acta 69, 4007–4034.

Martinez, C.E., McBride, M.B., Kandianis, M.T., Duxbury, J.M., Yoon, S., Bleam, W.F., 2002. Zinc_sulfur and cadmium-sulfur association in metalliferous peats: evidence from spectroscopy, distribution coefficients, and phytoavailability. Environ. Sci. Technol. 36, 3683–3689.

Marzouk, E.R., Chenery, S.R., Young, S.D., 2013. Predicting the solubility and lability of Zn, Cd, and Pb in soils from a minespoil-contaminated catchment by stable isotopic exchange. Geochim. Cosmochim. Acta 123, 1–16.

Methodological Recommendations of the Scientific Council on the Methods of Mineralogical Studies (no. 158. Moscow in Russian).

Michálková, Z., Komárek, M., Vítková, M., Řečínská, M., Ettler, V., 2016. Stability, transformations and stabilizing potential of an amorphous manganese oxide and its surface-modified form in contaminated soils. Appl. Geochem. 75, 125–136.

Miller, P.W., Martens, D.C., Zelazny, L.W., 1986. Effect of sequence in extraction of trace metals from soils. Soil Sci. Soc. Am. J. 50, 598–601.

Minkina, T.M., Soldatov, A.V., Motuzova, G.V., Podkovyrina, Yu.S., Nevidomskaya, D.G., 2014. Speciation of copper and zinc compounds in artificially contaminated chernozem by X-ray absorption spectroscopy and extractive fractionation. J. Geochem. Explor. 144, 306–311.

Minkina, T.M., Soldatov, A.V., Nevidomskaya, D.G., Motuzova, G.V., Podkovyrina, Yu.S., Mandzhieva, S.S., 2016. New approaches to studying heavy metals in soils by X-ray absorption spectroscopy (XANES) and extractive fractionation. Geochem. Int. 54 (2):197–204. https://doi.org/10.1134/S001670291512006X.

Minkina, T.M., Linnik, V.G., Nevidomskaya, D.G., Bauer, T.V., Mandzhieva, S.S., Khoroshavin, V.Y., 2017. Forms of Cu (II), Zn (II), and Pb (II) compounds in technogenically transformed soils adjacent to the Karabashmed copper smelter. J. Soils Sediments https://doi.org/10.1007/s11368-017-1708-2.

Myers, J., Thorbjornsen, K., 2004. Identifying metals contamination in soil: a geochemical approach. Soil Sediment Contam. 13, 1–16.

Nannoni, F., Protano, G., Riccobono, F., 2011. Fractionation and geochemical mobility of heavy elements in soils of a mining area in northern Kosovo. Geoderma (16), 63–73.

Nevidomskaya, D.G., Minkina, T.M., Soldatov, A.V., Shuvaeva, V.A., Zubavichus, Y.V., Podkovyrina, Yu.S., 2016. Comprehensive study of Pb (II) speciation in soil by X-ray absorption spectroscopy (XANES and EXAFS) and sequential fractionation. J. Soils Sediments 16 (4):1183–1192. https://doi.org/10.1007/s11368-015-1198-z.

Newville, M., 2001. IFEFFIT: interactive XAFS analysis and FEFF fitting. J. Synchrotron Radiat. 8, 322–324.

Perelman, A.I., Kasimov, N.S., 1999. Landscape Geochemistry. Asteya-2000, Moscow (in Russian).

Petruzzelli, G., Petronio, B.M., Gennaro, M.C., Vanni, A., Liberatori, A., Barbafieri, M., Pezzarossa, B., 1997. Residual effect of application of sewage sludge on heavy metals sorption by soil. Ann. Chim. 87 (11/12), 733–742.

Pinskii, D.L., 1998. The problem of the mechanisms of ion-exchange adsorption of heavy metals in soils. Eurasian Soil Sci. 31 (11), 1223–1230.

Pinskii, D.L., Minkina, T.M., 2013. Regularities of Cu, Pb and Zn adsorption by chernozems of the South of Russia. Eur. J. Soil Sci. 2, 59–68.

Pinskii, D.L., Minkina, T.M., Gaponova, Y.I., 2010. Comparative analysis of mono-and polyelement adsorption of copper, lead and zinc by an ordinary chernozem from nitrate and acetate solutions. Eurasian Soil Sci. 43, 748–756.

Privalenko, V.V., Mazurenko, V.T., Panaskov, V.I., Moshkin, V.M., Mukhin, N.V., Senin, B.K., 2000. Ecological Problems in the City of Kamensk-Shakhtinsk (Tsvetnaya pechat', Postov-on-Don in Russian).

Scheinost, A.C., Kretzchmar, R.S., Pfister, S., 2002. Combining selective sequential extractions, X-ray adsorption spectroscopy, and principal component analysis for quantitative zinc speciation in soil. Environ. Sci. Technol. 36, 5021–5028.

Schlegel, M.L., Manceau, A., Charlet, L., Chateigner, D., Hazemann, J.I., 2001. Sorption of metal ions on clay minerals. III. Nucleation and epitaxial growth of Zn phyllosilicate on the edges of hectorite. Geochim. Cosmochim. Acta 65, 4155–4170.

Shaheen, S.M., Rinklebe, J., Tsadilas, C.D., 2015. Fractionation and mobilization of toxic elements in floodplain soils from Egypt, Germany and Greece: a comparison study. Eurasian Soil Sci. 48 (12), 1317–1328.

Synchrotron-based techniques in soils and sediments. In: Singh, B., Gräfe, M. (Eds.), Developments in Soil Science. vol. 34. Elsevier B.V, Amsterdam.

Tessier, A., Campbell, P.G.C., Bisson, M., 1979. Sequential extraction procedure for the speciation of particulate trace metals. Anal. Chem. 51, 844–850.

Vinogradov, A.P., 1957. Geochemistry of Rare and Dispersed Chemical Elements in Soils. RAN, Moscow (in Russian).

Voegelin, A., Pfister, S., Scheinost, A.C., Marcus, M.A., Kretzshmar, R., 2005. Changes in zinc speciation in field soil after contamination with zinc oxide. Environ. Sci. Technol. 39 (17), 6616–6623.

Williams, J.G., McLaren, R.G., 1982. Effects of dry moist incubation of soils on the extractability of native and applied soil copper. Plant Soil 64 (2), 215–224.

Wisawapipat, W., Janlaksana, Y., Christl, L., 2017. Zinc solubility in tropical paddy soils: a multi-chemical extraction technique study. Geoderma 301, 1–10.

Young, S.D., Zhang, H., Tye, A.M., Maxted, A., Thums, C., Thornton, I., 2005. Characterizing the availability of metals in contaminated soils. I. The solid phase: sequential extraction and isotopic dilution. Soil Use Manag. 21, 450–458.

Zabinski, S.I., Rehr, J.J., Ankudinov, A., Alber, R.C., 1995. Multiple-scattering calculations of X-ray absorption spectra. Phys. Rev. B 52, 2995–3009.